Letter

Path Following of Underactuated Autonomous Surface Vessels With Surge Velocity Constraint and Asymmetric Saturation

Yalei Yu, Chen Guo, and Tieshan Li, *Senior Member, IEEE*

Dear Editor,

This letter is concerned with the path following of underactuated autonomous surface vessels (ASV) in the presence of surge velocity constraint and asymmetric saturation as well as unknown dynamics. To cope with velocity constraints both magnitude and rate and asymmetric saturation as well as unknown dynamics, an adaptive finite-time sliding mode control scheme (AFTSM) is designed. Then ASV's constraints could be addressed correspondingly by a novel rate and magnitude velocity guidance and projection-based finite-time auxiliary system and parametric finite-time robust observer in this scheme. Finally, the effective performance of the presented scheme is demonstrated via a series of simulations and comparisons.

Path following problem is researched widely throughout the control community due to its practical application both single and multi-agents in many areas [1]–[4]. In the guidance subsystem, the line-of-sight (LOS)-based guidance is the most common way to design guidance angle [5]–[10]. However, the finite-time observer in [10] suffers from fixed fractional power term, which loses flexibility in different systems. In addition, although the path curvature is considered in the sway dynamic analysis in [1], the effect of adding this factor in kinetic level is yet not studied. In the control subsystem, some researchers design velocity guidance by considering cross-tracking errors [10]–[12]. On the other hand, rate constraint of surge velocity caused by limited engine power in practice, which affects the performance especially in the acceleration period, attracts very limited attention. Although this problem has been considered in [13], the author does not consider the rate constraint and path curvature simultaneously.

Regarding the force and moment design, actuator saturation of ASV is caused by physical limitations, which is ubiquitous in practice [7], [10] and [14]–[19]. However, they only consider the symmetric saturation. To solve the constraints induced by non-symmetric saturation, there are some ways such as approximation-based approaches like tanh function in [20] and Gaussian error functions in [21], and a novel bounded saturation function [22]. But, these methods in [20]–[22] can not guarantee finite-time stability. Note that although error auxiliary systems are presented in [23], control auxiliary systems like [7] for asymmetric saturation have not been designed and analysed up to now, and the auxiliary state may suffer from parameter drift.

Motivated by the above observation, this letter aims to design an AFTSM scheme for ASV subject to velocity constraint, asymmetric saturation and uncertainties. Key novelties of this scheme lie in the following aspects: 1) On the basis of [10], a parametric finite-time robust observer is introduced in sideslip angle and unknown dynamic estimations, which features with flexibility for fractional power choices to be designed in specific system such as robot systems. 2) A novel rate and magnitude velocity guidance law integrated with path curvature of desired path is developed to cope with rate and magnitude constraints of surge velocity simultaneously via hyperbolic functions such that better performance is reached in comparison to [13], especially in turning sections. 3) Compared with literature [7] and [20]–[23], asymmetric saturation is studied thoroughly by designing projection-based finite-time auxiliary system, which works for symmetric case and performs expected performance, and thus the domain of auxiliary states can be strictly guaranteed within a finite settling time reducing parametric drift.

Problem formulation: The mathematical model of an ASV on a horizontal plane with kinematics and kinetics dynamics, is described as follows [24]: $\dot{\boldsymbol{\eta}} = \boldsymbol{J}(\psi)\boldsymbol{\nu}, \dot{\boldsymbol{\nu}} = \boldsymbol{f} + \boldsymbol{\tau}$ where $\boldsymbol{\eta} = [x, y, \psi]^T$, $\boldsymbol{\nu} = [u, v, r]^T$, $\boldsymbol{\tau} = [\tau_u/m_{11}, 0, \tau_r/m_{33}]^T$, $\tau_l = \tau_{l\mathrm{m}}^-, (l = u, r)$, if $\tau_{l0} < \tau_{l\mathrm{m}}^-$, otherwise $\tau_l = \mathrm{sgn}(\tau_{l0})\min\{|\tau_{l0}|, \tau_{l\mathrm{m}}^+\}$, and

$$\begin{bmatrix} f_u \\ f_v \\ f_r \end{bmatrix} = \begin{bmatrix} \dfrac{m_{22}}{m_{11}} vr - \dfrac{d_{11}}{m_{11}} u + \dfrac{(b_u \cos\psi + b_v \sin\psi)}{m_{11}} \\ -\dfrac{m_{11}}{m_{22}} ur - \dfrac{d_{22}}{m_{22}} v - \dfrac{d_{23}}{m_{22}} r + \dfrac{(b_v \cos\psi - b_u \sin\psi)}{m_{22}} \\ \dfrac{m_{11} - m_{22}}{m_{33}} uv - \dfrac{d_{32} v}{m_{33}} - \dfrac{d_{33}}{m_{33}} r + \dfrac{b_r}{m_{33}} \end{bmatrix}.$$

The objective of this letter is to design LOS-based guidance laws and control laws that force ASV to follow and stay on a reference path $\boldsymbol{\eta}_p(\theta)$, moving with developed surge velocity, such that position and velocity tracking errors of ASV converge to an arbitrarily small neighbourhood of zero within a finite time.

Assumption 1: The unknown time-varying sideslip angle β and its derivative $\dot{\beta}$ satisfy $|\beta| \le \beta^* < \infty$ and $|\dot{\beta}| \le \dot{\beta}^* < \infty$.

Main results: In this section, the AFTSM scheme is developed.

Recall the finite-time LOS (FTLOS) guidance laws in [10]

$$\begin{cases} \psi_d = \gamma_p + \arctan(-(y_e + k_y \mathrm{sig}^{\rho}(y_e) + \Delta\hat{\beta})/\Delta) \\ u_\theta = k_0 x_e + k_1 \mathrm{sig}^{\rho}(x_e) + U\cos(e_\psi) - U\sin(e_\psi)\hat{\beta} \end{cases} \tag{1}$$

where Δ is a look-ahead distance, $\mathrm{sig}^{\rho}(\star) = |\star|^{\rho}\mathrm{sgn}(\star)$ [4], [25], and $k_y \in \mathbb{R}_+$. $(k_0, k_1) \in \mathbb{R}_+^2$. $\dot{\theta} = u_\theta / \sqrt{\dot{x}_p^2 + \dot{y}_p^2}$. The sideslip angle is estimated by the parametric finite-time robust observer

$$\begin{cases} \dot{\hat{y}}_e = -k_{\beta 1}\mathrm{sig}^{\alpha}(\tilde{y}_e) + \hat{h} + \tau_\beta \\ \dot{\hat{h}} = -k_{\beta 2}\mathrm{sig}^{2\alpha-1}(\tilde{y}_e) - \vartheta_\beta \mathrm{sgn}(\tilde{y}_e) \end{cases} \tag{2}$$

where $h = U\cos(e_\psi)\beta$, $\tau_\beta = -\dot{\gamma}_p x_e + U\sin(e_\psi)$ and $(\lambda_{\beta 0}, \lambda_\beta) \in \mathbb{R}_+^2$; $\hat{y}_e$ and $\hat{h}$ are the estimates of y_e and h, respectively, satisfying $\tilde{y}_e = \hat{y}_e - y_e$ and $\tilde{h} = \hat{h} - h$, thus, $\hat{\beta} = \hat{h}/U\cos(e_\psi)$.

To stabilize ASV's attitude, design virtual yaw angle and moment

$$\begin{cases} r_d = -k_{\psi 0}\psi_e + \dot{\psi}_d - k_{\psi 1}\mathrm{sig}^{\rho}(\psi_e) \\ \tau_{r0} = -m_{33}[\hat{f}_r - \dot{r}_d + (\alpha_r r_e + \beta_r r_e \mathrm{sig}^{\rho}(r_e))] \\ \qquad + k_{r0}\chi_r - \lambda_r S_r - \xi_r \mathrm{sig}^{\rho}(S_r) \end{cases} \tag{3}$$

where $(k_{\psi 0}, k_{\psi 1}, k_{r0}, \lambda_r, \xi_r, \alpha_r, \beta_r) \in \mathbb{R}_+^7$, $S_r = r_e + \int_0^t (\alpha_r r_e + \beta_r \mathrm{sig}^{\rho}(r_e))\mathrm{d}\tau$, and $r_e = r - r_d$. $\hat{f}_r$ and χ_r will be designed later. A so-called finite-time tracking differentiator method is employed to generate $\dot{r}_d$ as follows [26]: $\dot{r}_{d1} = r_{d2}$, $\dot{r}_{d2} = -\varrho^2[k_{d1}\mathrm{sig}^{\rho_0}(r_{d1} - r_d) + k_{d2}\mathrm{sig}^{\rho_1}(r_{d2}/\varrho)]$ where $(\rho_0, \rho_1, k_{d1}, k_{d2}) \in \mathbb{R}_+^4$, r_{d1} and r_{d2} are estimates of r_d and $\dot{r}_d$, respectively.

To stabilize ASV's surge velocity, design rate and magnitude velocity guidance and nominal surge force τ_{u0} as follows:

Corresponding author: Yalei Yu and Chen Guo.

Citation: Y. L. Yu, C. Guo, and T. S. Li, "Path following of underactuated autonomous surface vessels with surge velocity constraint and asymmetric saturation," *IEEE/CAA J. Autom. Sinica*, vol. 10, no. 5, pp. 1343–1345, May 2023.

Y. L. Yu is with the School of Marine Electrical Engineering, Dalian Maritime University, Dalian 116026, China, and also with the Department of Aeronautical and Automotive Engineering, Loughborough University, Loughborough LE11 3RH, UK (e-mail: yuyalei89@gmail.com).

C. Guo is with the School of Marine Electrical Engineering, Dalian Maritime University, Dalian 116026, China (e-mail: guoc@dlmu.edu.cn).

T. S. Li is with the School of Automation Engineering, University of Electronic Science and Technology of China, Chengdu 611731, and also with the School of Navigation, Dalian Maritime University, Dalian 116026, China (e-mail: tieshanli@126.com).

Color versions of one or more of the figures in this paper are available online at http://ieeexplore.ieee.org.

Digital Object Identifier 10.1109/JAS.2023.123168

$$\begin{cases} u_d = u_{\max}\tanh(\alpha_u/u_{\max}) \\ \dot{\alpha}_u = \alpha_{\max}\tanh((k_{\alpha 3}\alpha_{ud} - k_{\alpha 3}\alpha_u)/\alpha_{\max}) \\ \alpha_{ud} = u_{\max}\tanh^{-1}((k_{\alpha 0}y_e^2 + u_0)/(u_{\max}e^{k_{\alpha 1}|K|+k_{\alpha 2}})) \\ \tau_{u0} = -m_{11}[\hat{f}_u - \dot{u}_d + (\alpha_u u_e + \beta_u \mathrm{sig}^{\rho}(u_e))] \\ \qquad + k_{u0}\chi_u - \lambda_u S_u - \xi_u \mathrm{sig}^{\rho}(S_u) \end{cases} \tag{4}$$

where $(k_{\alpha 0}, k_{\alpha 1}, k_{\alpha 2}, k_{\alpha 3}, k_{u0}, \lambda_u, \xi_u, \alpha_u, \beta_u) \in \mathbb{R}_+^9$, and K denotes path curvature. u_0, $u_{\max}$ and $\alpha_{\max}$ are positive constants. $S_u = u_e + \int_0^t (\alpha_u u_e + \beta_u \mathrm{sig}^{\rho}(u_e))\mathrm{d}\tau$, $u_e = u - u_d$. $\hat{f}_l$ is estimated by parametric finite-time robust observer as follows:

$$\begin{cases} \dot{\hat{l}} = -k_{l1}\mathrm{sig}^{\alpha}(\tilde{l}) + \hat{f}_l + \tau_l/m_l \\ \dot{\hat{f}}_l = -k_{l2}\mathrm{sig}^{2\alpha-1}(\tilde{l}) - \vartheta_l \mathrm{sgn}(\tilde{l}) \end{cases} \tag{5}$$

where $(k_{l1}, k_{l2}, \vartheta_l) \in \mathbb{R}_+^3$ $\tilde{l} = \hat{l} - l$, $\tilde{f}_l := \hat{f}_l - f_l$ and $m_u = m_{11}$ and $m_r = m_{33}$. To analyse input saturation, χ_l is designed via projection-based finite-time auxiliary system as follows:

$$\begin{cases} \dot{\chi}_l = \mathrm{Proj}(\chi_l, \Theta_l(\chi_l)) \\ \Theta_l = -k_{\chi l1}\chi_l - k_{\chi l2}\mathrm{sig}^{\rho}(\chi_l) + \rho_l \Delta\tau_l \\ \qquad - \dfrac{|S_l \Delta\tau_l| + 0.5\rho_l^2 \Delta\tau_l^2}{\chi_l} h(\chi_l) \end{cases} \tag{6}$$

where $\left(k_{\chi l1}, k_{\chi l2}, \rho_l\right) \in \mathbb{R}_+^3$, $\Delta\tau_l = \tau_l - \tau_{l0}$ and $h(\chi_l)$ is given in [10]. The Proj denotes the "smooth projection operator" [27].

Theorem 1: Consider the ASV, satisfying Assumption 1, and the FTLOS guidance law (1) and (2), yaw angle and moment (3), rate and magnitude velocity guidance and surge force (4), parametric finite-time robust observers (5), and projection-based finite-time auxiliary systems (6) are applied in AFTSM. Hence, one can tune the positive design parameters properly such that all error signals in the closed-loop guidance-control system are bounded in a small range and satisfy practical finite-time stability.

Proof: Consider the following augmented Lyapunov function candidate $V = x_e^2/2 + y_e^2/2 + m_{33}S_r^2/2 + \chi_r^2/2 + m_{11}S_u^2/2 + \chi_u^2/2$. Differentiate V in virtue of (1)–(6) with respect to time, and V_θ in [10], for all $T_Y \le t$, results can be obtained as follows:

$$\begin{aligned} \dot{V} \le & -k_0\theta_1^0 x_e^2 - k_1\theta_1^1 (x_e^2)^{\rho_*} - \omega_1^* y_e^2 - \omega_2^* (y_e^2)^{\rho_*} + \kappa_v \\ & - \left(k_{\chi r1} - 0.5k_{r0} - 0.5\right)\chi_r^2 - k_{\chi r2}(\chi_r^2)^{\rho_*} - \xi_r\left(S_r^2\right)^{\rho_*} \\ & - (\lambda_u - 0.5k_{u0})S_u^2 - \xi_u (S_u^2)^{\rho_*} - k_{\chi u2}(\chi_u^2)^{\rho_*} \\ & - (k_{\chi u1} - 0.5k_{u0} - 0.5)\chi_u^2 - (\lambda_r - k_{r0}/2)S_r^2 \\ \le & -\varsigma_1 V - \varsigma_2 V^{\rho_*} + \kappa_v \end{aligned} \tag{7}$$

where $\kappa_v = 0.5(\rho_r^2\Delta\tau_r^2(1 - h(\chi_r)) + 0.5\rho_u^2\Delta\tau_u^2(1 - h(\chi_u)) + |\Delta\tau_r S_r| \times (\mathrm{sgn}(\Delta\tau_r S_r) - h(\chi_r)) + |\Delta\tau_u S_u|(\mathrm{sgn}(\Delta\tau_u S_u) - h(\chi_u))$, $\rho_* = (\rho + 1)/2$ and $\varsigma_1 = 2\min\{k_0\theta_1^0, \omega_1^*, \lambda_r - 0.5k_{r0} - 0.5, k_{\chi r1}\chi_r^* - 0.5k_{r0} - 0.5\chi_r^*, \lambda_u - 0.5k_{u0} - 0.5, k_{\chi u1}\chi_u^* - 0.5k_{u0} - 0.5\chi_u^*\}$, $\varsigma_2 = 2^{\rho_*}\min\{k_1\theta_1^1, \omega_2^*, \xi_r, k_{\chi r2}, \xi_u, k_{\chi u2}\}$. When $h(\chi_l) = 1$, i.e., $\chi_l \ge b$, $\kappa_v = 0$ holds, and otherwise $h(\chi_l) < 1$, i.e., $\chi_l < b < \infty$, from the auxiliary system (6), we know $\Delta\tau_l$ is also bounded satisfying $\Delta\tau_l \le \Delta\tau_{lM} < \infty$, and thus $\kappa_v \le (\Delta\tau_{rM}^2 + \Delta\tau_{uM}^2 + \rho_r^2\Delta\tau_{rM}^2 + \rho_u^2\Delta\tau_{uM}^2)/2$, noting that coefficients of S_l^2 add 0.5 in this case. There exist a constant $0 < \theta_v < 1$ such that the following inequalities hold:

$$\dot{V} \le -\varsigma_1\theta_v V - \varsigma_2 V^{\rho_*}, \text{ or, } \dot{V} \le -\varsigma_1 V - \varsigma_2\theta_v V^{\rho_*}. \tag{8}$$

Using the Lemma 4 in [10], the finite-time stability is guaranteed for the guidance-control system of ASV, and V can converge to the following region $\Omega_v := \{\lim_{t\to T_v}|V \le \min\{\kappa_v/((1-\theta_v)\varsigma_{v1}), (\kappa_v/(1-\theta_v)\varsigma_{v2})^{2/(\rho+1)}\}\}$ within a finite time as follows: $T_v \le \max\{t_0 + \frac{1}{\theta_v\varsigma_1\phi}\ln\frac{\theta_v\varsigma_1 V^{\phi}(t_0)+\varsigma_2}{\varsigma_2}, t_0 + \frac{1}{\varsigma_1\phi}\ln\frac{\varsigma_1 V^{\phi}(t_0)+\theta_v\varsigma_2}{\theta_v\varsigma_2}\}$, where $\phi = (1-\rho)/2$. Therefore, the practical finite-time stability for error signals $\tilde{\beta}, x_e, y_e, \psi_e, S_u$ and S_r is guaranteed, and thus boundedness of u_e and r_e is produced within T_v along with (3) and (4). Consequently, all error signals of the closed-loop guidance-control system of ASV satisfy practical finite-time stability and converge to an arbitrarily small region by choosing controller design parameters approximately. ■

Numerical example: Simulation studies are conducted with the ASV [10]. The maximum surge force is set approximately $\tau_{um}^+ = 5$ N and the minimum $\tau_{um}^- = -3$ N, and the maximum moment is set approximately $\tau_r^+ = -\tau_{rm}^- = 3.5\ \mathrm{N}\cdot\mathrm{m}$. The initial conditions are given by $[x(0), y(0), \psi(0)] = [0\ \mathrm{m}, 20\ \mathrm{m}, 1/3\ \mathrm{rad}]$, $[u(0), v(0), r(0)] = [0.1\ \mathrm{m/s}, 0\ \mathrm{m/s}, 0\ \mathrm{rad/s}]$. The design parameters are $k_y = 1.2$, $k_0 = 1$, $k_1 = 2$, $k_{\beta 1} = 38$, $k_{\beta 2} = 0.5$, $\vartheta_\beta = 0.01$, $\vartheta_l = 0.01$, $k_{l1} = 2$, $k_{l2} = 5$, $\rho = 0.8$, $k_{\psi 0} = 0.6$, $k_{\psi 1} = 0.1$, $k_{r0} = 10$, $\lambda_l = 2$, $\xi_l = 1$, $\alpha_r = 1.5$, $\alpha_u = 5$, $\beta_l = 0.1$, $k_{\alpha 0} = 3$, $k_{\alpha 1} = 10$, $k_{\alpha 2} = 0.1$, $k_{\alpha 3} = 1$, $\rho_0 = 0.1$, $\rho_1 = 0.8$, $k_{d1} = 0.2$, $k_{d2} = 20$, $k_{u0} = 10$, $u_0 = 1$, $u_{\max} = 2$, $k_{\chi l1} = 0.2$, $k_{\chi l2} = 1$, $\rho_l = 1$, $a = 0.1$, $b = 0.5$, $\alpha = \{0.6, 0.8, 0.95\}$. The desired path is given by $y_p(\theta) = 10\sin(0.1x_p(\theta))$. For the design of ocean disturbances and bidirectional step jump signals, please see [10].

To prove the effectiveness of the proposed scheme, a series of comparative simulation studies are conducted. There are seven sets for simulation studies, that are, the AFTSM scheme, the AFTSM without considering rate and curvature constraints marked as AFTSMWCR, the AFTSM without path curvature only marked as AFTSMWCO, the AFTSM without rate constraints marked as AFTSMWRO, the AFTSM without projection algorithm marked as AFTSMWPROJ, the AFTSM with $\alpha = 0.6$ marketed as AFTSMAL06, and the AFTSM with $\alpha = 0.95$ marketed as AFTSMAL095, with the same design parameters.

The comparative results plotted in Figs. 1−3 demonstrate that the AFTSM provides effective performance. The Fig. 1 displays the performance of path following among these seven sets, and obviously, the AFTSM provides accurately fast tracking by comparing with other sets, and better transient tracking performance both the initial and turning periods. It can be observed that along-track and cross-track errors converge to the vicinity of zero later due to considering rate constraint and path curvature together depicted in Fig. 2, whereas the presented AFTSM shows better performance for convergence of velocity errors, which plays a key role in engineering application. In this figure, the comparison of different fractional power terms in parametric finite-time robust observer reveals that when $\alpha = 0.6$, the worst is seen, and when $\alpha = 0.8$, the results are better than $\alpha = 0.95$. This means the performance may become bad with the increase of α after it reaches a certain value. From the Fig. 3 , the effectiveness of introducing projection algorithm in auxiliary system is illustrated with better convergence for auxiliary states and tracking errors as well as reducing parametric drift. This figure also shows the strong robustness of the AFTSM control scheme when it suffers from measurement noises and disturbances in the form of bidirectional step jump signals. It is worth mentioning that when the velocity guidance does not consider rate or curvature (or both), the significant fluctuation shows for $\hat{f}_u$ and corresponding τ_u. This is caused by the rapid change in the fast turning periods, and thus obviously the proposed AFTSM algorithm performs well in this sort of tough sailing situations.

Conclusion: A novel AFTSM control scheme is presented for path following of ASV under surge velocity constraint, asymptotic saturation, and unknown dynamics. All signals in the closed-loop system of ASV satisfy practical finite-time stability proved by simulations.

Acknowledgments: This work was supported by the National Natural Science Foundation of China (51879027, 51939001, 61976033, 51579024, 61374114, 51809028), the Liaoning Revitalization Tal-

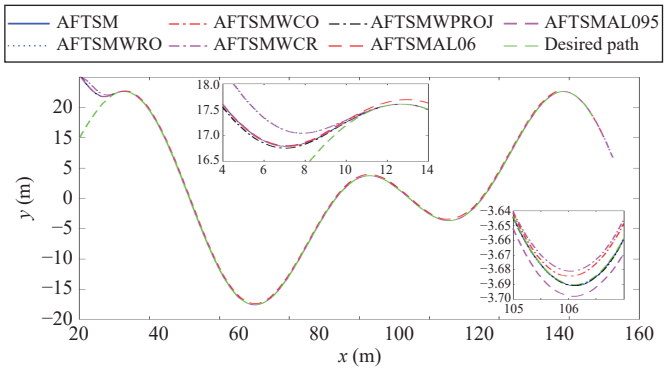

Fig. 1. Path following performance.

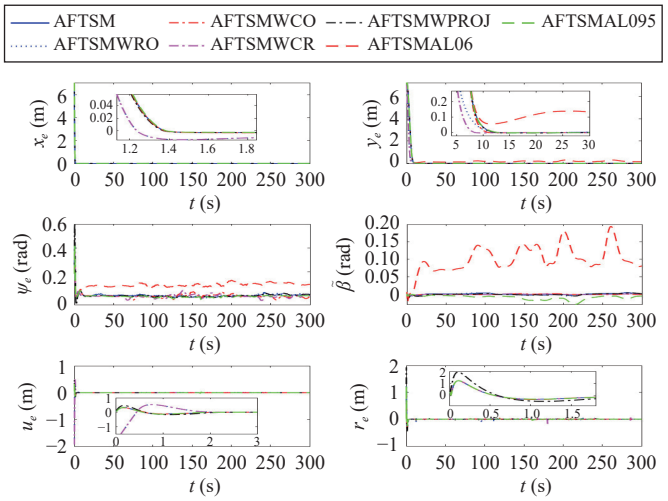

Fig. 2. Position, attitude and velocity errors.

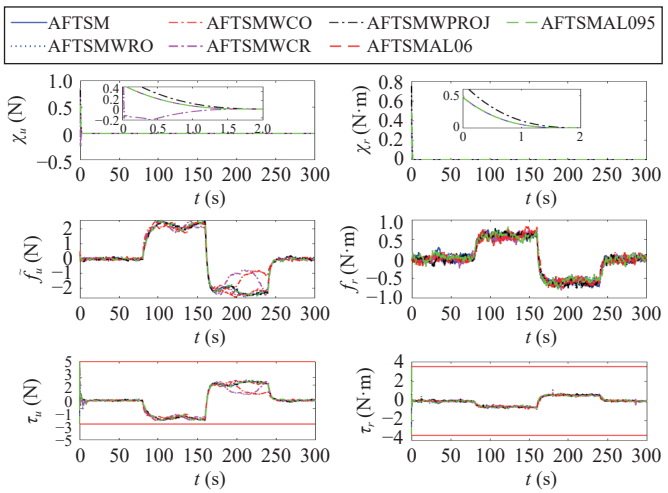

Fig. 3. Auxiliary states, estimation errors and control laws.

ents Program (XLYC1908018), the Natural Foundation Guidance Plan Project of Liaoning (2019-ZD-0151), the Cultivation Program for the Excellent Doctoral Dissertation of Dalian Maritime University, and the Fundamental Research Funds for the Central Universities (3132019318, 3132019345).

References

[1] D. Belleter, M. A. Maghenem, C. Paliotta, and K. Y. Pettersen, "Observer based path following for underactuated marine vessels in the presence of ocean currents: A global approach," *Automatica*, vol. 100, pp. 123–134, 2019.

[2] Z. Peng, J. Wang, D. Wang, and Q.-L. Han, "An overview of recent advances in coordinated control of multiple autonomous surface vehicles," *IEEE Trans. Industrial Informatics*, vol. 17, no. 2, pp. 732–745, 2021.

[3] N. Gu, D. Wang, Z. Peng, J. Wang, and Q.-L. Han, "Recent advances in line-of-sight guidance for path following of autonomous marine vehicles: An overview," *IEEE Trans. Systems, Man, Cybernetics: Systems*, vol. 53, no. 1, pp. 12–28, 2023.

[4] T. Li, R. Zhao, C. P. Chen, L. Fang, and C. Liu, "Finite-time formation control of under-actuated ships using nonlinear sliding mode control," *IEEE Trans. Cybernetics*, vol. 48, no. 11, pp. 3243–3253, 2018.

[5] S. R. Oh and J. Sun, "Path following of underactuated marine surface vessels using line-of-sight based model predictive control," *Ocean Engineering*, vol. 37, pp. 289–295, 2010.

[6] L. Liu, D. Wang, and Z. Peng, "ESO-based line-of-sight guidance law for path following of underactuated marine surface vehicles with exact sideslip compensation," *IEEE J. Oceanic Engineering*, vol. 42, no. 2, pp. 477–487, 2017.

[7] Z. Zheng and M. Feroskhan, "Path following of a surface vessel with prescribed performance in the presence of input saturation and external disturbances," *IEEE/ASME Trans. Mechatronics*, vol. 22, no. 6, pp. 2564–2575, 2017.

[8] T. I. Fossen, K. Y. Pettersen, and R. Galeazzi, "Line-of-sight path following for dubins paths with adaptive sideslip compensation of drift forces," *IEEE Trans. Control Syst. Technology*, vol. 23, no. 2, pp. 820–827, 2015.

[9] Y. Yu, C. Guo, and H. Yu, "Finite-time PLOS-based integral sliding-mode adaptive neural path following for unmanned surface vessels with unknown dynamics and disturbances," *IEEE Trans. Automation Science Engineering*, vol. 16, no. 4, pp. 1500–1511, 2019.

[10] Y. Yu, C. Guo, and T. Li, "Finite-time LOS path following of unmanned surface vessels with time-varying sideslip angles and input saturation," *IEEE/ASME Trans. Mechatronics*, vol. 27, no. 1, pp. 463–474, 2022.

[11] E. Peymani and T. I. Fossen, "Speed-varying path following for underactuated marine craft," *IFAC Proc. Volumes*, vol. 46, no. 33, pp. 79–84, 2013.

[12] K. D. Do, Z. P. Jiang, and J. Pan, "Robust adaptive path following of underactuated ships," *Automatica*, vol. 40, no. 6, pp. 929–944, 2004.

[13] M. Breivik, V. E. Hovstein, and T. I. Fossen, "Straight-line target tracking for unmanned surface vehicles," *Modeling, Identification Control*, vol. 29, no. 4, pp. 131–149, 2008.

[14] Z. Peng, J. Wang, and Q.-L. Han, "Path-following control of autonomous underwater vehicles subject to velocity and input constraints via neurodynamic optimization," *IEEE Trans. Industrial Electronics*, vol. 66, no. 11, pp. 8724–8732, 2019.

[15] T. Li, R. Li, and J. Li, "Decentralized adaptive neural control of nonlinear interconnected large-scale systems with unknown time delays and input saturation," *Neurocomputing*, vol. 74, no. 14–15, pp. 2277–2283, 2011.

[16] Y. Yang, J. Tan, and D. Yue, "Prescribed performance control of one-dof link manipulator with uncertainties and input saturation constraint," *IEEE/CAA J. Autom. Sinica*, vol. 6, no. 1, pp. 148–157, 2019.

[17] N. Zerari, M. Chemachema, and N. Essounbouli, "Neural network based adaptive tracking control for a class of pure feedback nonlinear systems with input saturation," *IEEE/CAA J. Autom. Sinica*, vol. 6, no. 1, pp. 278–290, 2019.

[18] Y. Su, Q. Wang, and C. Sun, "Self-triggered consensus control for linear multi-agent systems with input saturation," *IEEE/CAA J. Autom. Sinica*, vol. 7, no. 1, pp. 150–157, 2020.

[19] M. Chen, S. S. Ge, and B. V. E. How, "Robust adaptive neural network control for a class of uncertain MIMO nonlinear systems with input nonlinearities," *IEEE Trans. Neural Networks*, vol. 21, no. 5, pp. 796–812, 2010.

[20] Z. Zheng, Y. Huang, L. Xie, and B. Zhu, "Adaptive trajectory tracking control of a fully actuated surface vessel with asymmetrically constrained input and output," *IEEE Trans. Control Syst. Technology*, vol. 26, no. 5, pp. 1851–1859, 2018.

[21] Z. Li and J. Zhao, "Adaptive consensus of non-strict feedback switched multi-agent systems with input saturations," *IEEE/CAA J. Autom. Sinica*, vol. 8, no. 11, pp. 1752–1761, 2021.

[22] J. Zhang, X. Xiang, Q. Zhang, and W. Li, "Neural network-based adaptive trajectory tracking control of underactuated AUVs with unknown asymmetrical actuator saturation and unknown dynamics," *Ocean Engineering*, vol. 218, p. 108193, 2020.

[23] Y. Gao, X. Sun, C. Wen, and W. Wang, "Observer-based adaptive nn control for a class of uncertain nonlinear systems with nonsymmetric input saturation," *IEEE Trans. Neural Networks Learning Syst.*, vol. 28, no. 7, pp. 1520–1530, 2017.

[24] T. I. Fossen, *Handbook of Marine Craft Hydrodynamics and Motion Control*, 1st ed. Trondheim, Norway: John Wiley & Sons, 2011.

[25] S. Yu, X. Yu, B. Shirinzadeh, and Z. Man, "Continuous finite-time control for robotic manipulators with terminal sliding mode," *Automatica*, vol. 41, no. 11, pp. 1957–1964, 2005.

[26] Z. Peng, D. Wang, T. Li, and M. Han, "Output-feedback cooperative formation maneuvering of autonomous surface vehicles with connectivity preservation and collision avoidance," *IEEE Trans. Cybernetics*, vol. 50, no. 6, pp. 2527–2535, 2020.

[27] Z. Cai, M. S. DeQueiroz, and D. M. Dawson, "A sufficiently projection operator," *IEEE Trans. Automatic Control*, vol. 51, no. 1, pp. 135–139, 2006.